iScience

CellPress
OPEN ACCESS

Article

Evidence in Support of the Border-Ownership Neurons for Representing Textured Figures

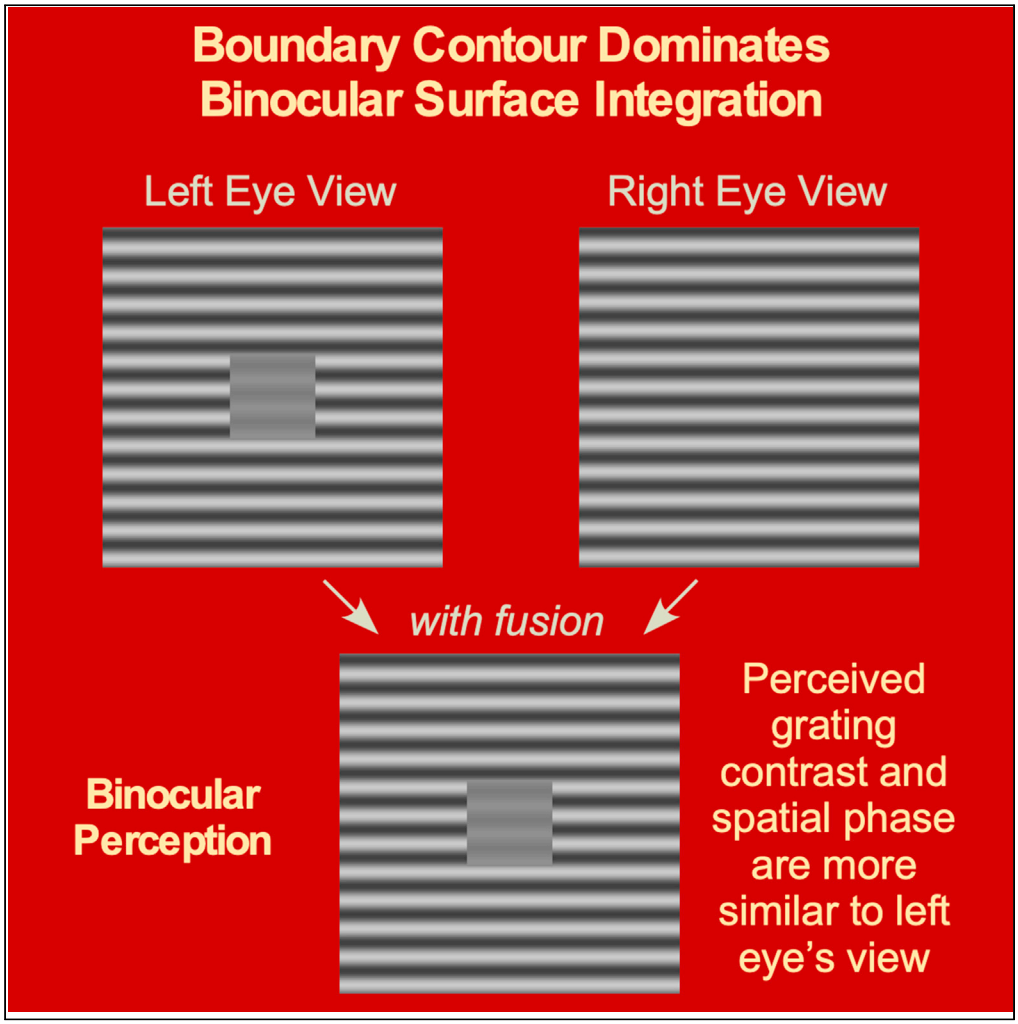

Chao Han, Wanyi Huang, Yong R. Su, Zijiang J. He, Teng Leng Ooi

zjhe@louisville.edu (Z.J.H.)
ooi.22@osu.edu (T.L.O.)

HIGHLIGHTS

Psychophysical evidence for a border-to-interior coding scheme in binocular vision

Boundary contour (BC) plays a leading role in integrating dichoptic texture images

Image with stronger BC in one eye contributes more to binocular texture integration

The eye seeing the stronger BC image exerts stronger suppression on the fellow eye

Han et al., iScience *23*, 101394
August 21, 2020
https://doi.org/10.1016/j.isci.2020.101394

iScience

CellPress
OPEN ACCESS

Article

Evidence in Support of the Border-Ownership Neurons for Representing Textured Figures

Chao Han,[1] Wanyi Huang,[1] Yong R. Su,[2] Zijiang J. He,[2,*] and Teng Leng Ooi[1,3,*]

SUMMARY

We presented one eye with a monocular-boundary-contour (MBC) square, created by phase-shifting a central region of grating relative to a larger uniform grating surround, and the fellow eye with the larger uniform grating. In addition, the grating within the MBC region was rendered with lower contrast relative to the remaining stimulus. Despite this, we found the lower contrast MBC region dominated the perceived cyclopean contrast, with the corresponding region in the fellow eye being suppressed. Secondly, we found for dichoptic stimuli with half-images having square grating regions of different BC strengths, the interocular BC strength ratio determined the perceived contrast of the cyclopean square. Thirdly, we found perceived spatial phase of the cyclopean square was dominated by the spatial phase of the MBC half-image. Altogether, these psychophysical findings provided evidence for a border-to-interior representation strategy, that constructing surface begins at the boundary contour (BC), in binocular contrast and phase integration.

INTRODUCTION

The binocular visual mechanism represents three-dimensional (3-D) surfaces by utilizing the difference in visual scene perspectives imaged on the two retinas. But beyond this certainty, it is unclear how the visual system integrates the two retinal perspectives into a veridical surface representation of the 3-D scene. In theory, there are two computational strategies, either by integrating the local contrast information (*region-based coding* strategy) or by globally extracting the boundary contours (BC) of the surface image followed by the filling in of the local contrast information (*border-to-interior representation* strategy) (Grossberg and Mingolla, 1985; Julesz, 1960; Mumford et al., 1987; Paradiso and Nakayama, 1991). The *region-based coding* strategy could be implemented in the primary visual cortex where the early filtering processes exist (e.g., orientation and spatial frequency selective neurons). Consider the dichoptic grating stimulus in Figure 1A. According to the *region-based coding* strategy, the visual system begins by integrating the local contrast signals from the two eyes and then spatially groups these signals as a surface. Indeed, this hypothesis has gained much support from empirical and modeling studies, particularly from those using random-dot stereograms (RDS) that are devoid of global BC and object information and those using binocular stimuli with equal BC strength in the two eyes (Ding and Sperling, 2006; Georgeson et al., 2016; Halpern and Blake, 1988; Julesz, 1960; Legge and Gu, 1989; Marr and Poggio, 1976; Ohzawa et al., 1990; Poggio and Fischer, 1977).

In contrast, there are fewer empirical studies investigating the *border-to-interior representation* strategy, although those that did have shed important insights on the roles of extrastriate cortical mechanisms in representing BC and stereoscopic edges (Bakin et al., 2000; Duncan et al., 2000; Hesse and Tsao, 2016; Qiu and von der Heydt, 2005; von der Heydt, 2015; von der Heydt and Zhang, 2018; von der Heydt et al., 2000; Williford and von der Heydt, 2016; Zhou et al., 2000). Specifically, Zhou et al. (2000) discovered a large percentage of macaque V2 neurons signaling border ownership of 2-D texture-free surface/figure in a manner mainly consistent with Gestalt rules. Furthermore, the border-ownership selective neurons' responses could be affected by the image's context that was located beyond the classical receptive fields of V2 neurons, suggesting that they were modulated by feedback signals representing larger surface areas. Critically, Qiu and von der Heydt (Qiu and von der Heydt, 2005) also found the V2 neurons' depth sign of border ownership was consistent with their depth sign revealed with RDS (Qiu and von der Heydt, 2005; von

[1]College of Optometry, The Ohio State University, Columbus, OH 43210, USA

[2]Department of Psychological and Brain Sciences, University of Louisville, Louisville, KY 40292, USA

[3]Lead Contact

*Correspondence: zjhe@louisville.edu (Z.J.H.), ooi.22@osu.edu (T.L.O.)

https://doi.org/10.1016/j.isci.2020.101394

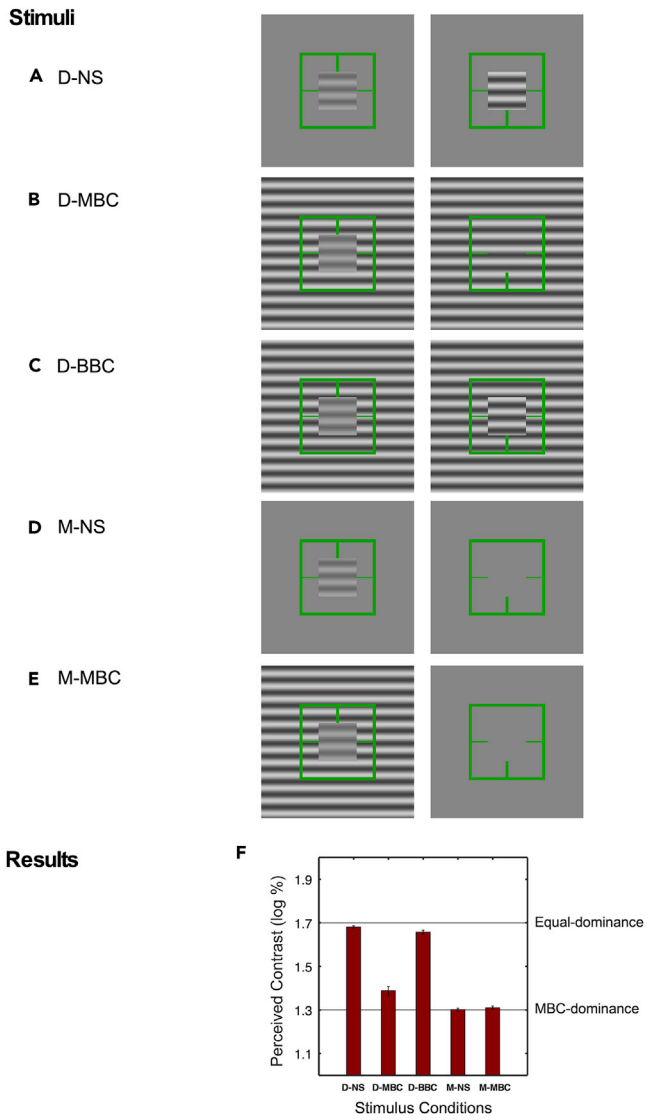

Figure 1. Experiment 1: Influence of BC on Binocular Contrast Integration

(A–E) The five stimulus conditions (see Transparent Methods and Table S1 for detailed descriptions).

(F) Average results (n = 5) showing the average perceived binocular contrast in the five conditions. Notably, perceived contrast is significantly higher in the D-NS condition than D-MBC condition, indicating the role of BC. We defined perceived contrast in log unit. Therefore, the labeled y axis values of 1.9, 1.7, 1.5, 1.3, and 1.1 correspond, respectively, to 79.4%, 50.1%, 31.6%, 20.0%, and 12.6%. The error bars represent standard errors of the mean.

der Heydt et al., 2000). This indicates the global depth determination based on Gestalt rules and local stereoscopic depth signals converge on the border-ownership selective neurons in V2.

An important implication of von der Heydt and colleagues' studies is that the *border-to-interior representation* strategy is implemented at the extrastriate cortices. However, this speculation requires further empirical evidence. This is because most neurophysiological studies of border-ownership selectivity of the V2 neurons employed texture-free (uniform color) figures, where only the figures' BCs (edges) carried the figural information. There are only two recent studies that revealed border-ownership selective neurons could also respond to natural stimuli such as to single faces and occluding faces (Hesse and Tsao, 2016) and to complex natural scenes (Williford and von der Heydt, 2016) with both BCs and interior textures. However, it remains unknown how the border-ownership selective neurons interact with neurons selective for local textures to form a global surface representation. To address this, the current study provided behavioral

evidence for the *border-to-interior representation* strategy by testing images with interior features (gratings). Our psychophysical experiments confirmed a prediction of the *border-to-interior representation* strategy that binocular surface perception of pattern and contrast is significantly affected by the relative BC strengths of the dichoptic stimulus.

RESULTS

To represent the binocular surface in Figure 1A, the visual system can interocularly integrate the local contrast signals and then spatially group them as a surface (Ding and Sperling, 2006; Georgeson et al., 2016; Halpern and Blake, 1988; Legge and Gu, 1989). With this *region-based coding* strategy, the perceived cyclopean contrast of the binocular surface depends only on the contrast of the gratings in each half-image. However, if the visual system adopts the *border-to-interior representation* strategy, the BC signals from the two eyes will first be integrated according to their relative strength. From the integrated binocular BC, the grating texture is sequentially added by a "filling-in" process whereby local grating patches adjacent to the BC spread inward until the entire area within the BC is filled. Importantly, the relative strength of the BC signals is the factor determining how the grating textures from the two eyes are integrated. Specifically, a stronger BC in one eye will lead to its grating texture carrying a larger weight when integrating with the grating texture from the fellow eye.

Experiment 1 directly investigated the role of the BC by testing whether the contrast of a half-image with BC contributed more to contrast perception over the half-image without the BC (see Figure 1B). The stimulus in Figure 1B differs from that in Figure 1A in one critical aspect, in that the former has BC in one half-image, whereas the latter has BCs in both half-images. In Figure 1A, the gratings in the left and right half-images, respectively, have +45° and −45° phase relative to the horizontal green reference lines. (We define 0° phase as that when the darkest horizontal zone of the grating aligns with the green reference lines, and a positive or negative phase indicates the darkest zone either being above or below the reference lines, respectively). The two gratings also differ in contrast (1.3 versus 1.7 log unit). With free fusion, one perceives the contrast of the cyclopean grating resembling that of the right half-image's (1.7 log unit). For simplicity, we call this a Dichoptic-with-No-Surround (D-NS) stimulus. Previous modeling works posit the perceived cyclopean contrast of D-NS stimulus is accounted for by an interocular contrast gain control mechanism (Ding et al., 2013; Ding and Sperling, 2006; Hou et al., 2013; Huang et al., 2010). To investigate the influence of BC, our new stimulus in Figure 1B added a high-contrast surround grating with −45° phase shift relative to a pair of green reference lines (Table S1). Accordingly, a monocular boundary contour (MBC) square is created in the left half-image of Figure 1B, due to the 90° phase difference between the central and surrounding gratings. There is no BC in the right half-image. We call this a Dichoptic-grating-with-MBC (D-MBC) stimulus. In Figure 1C, we added a surround grating with 180° phase, which causes the phase difference between the central and surround gratings to be 135° in both eyes. Since both half-images have BC, we called it a Dichoptic-with-Binocular Boundary Contours (D-BBC) stimulus.

We hypothesized that if BC significantly contributed to interocular contrast integration, then perceived cyclopean contrast of the central square would not be the same for all three stimuli. Specifically, if a preference existed for representing BC, then the lower contrast of the MBC grating in the D-MBC stimulus would have a larger contribution leading to lower perceived cyclopean contrast, unlike those of D-NS and D-BBC with BC in both eyes (leading to higher perceived contrast). One can qualitatively confirm this by free fusing the stimuli in Figures 1A–1C (Note that in both Figures 1B and 1C, the BCs of the larger grating square in each half-image have the same strength in the two eyes. Therefore, these BCs are unlikely to affect the interocular contrast integration that occurs in the center). We verified these observations empirically using a suprathreshold contrast matching task wherein observers matched the contrast of the test stimulus (D-NS, D-MBC, or D-BBC) with a standard matching stimulus. The matching stimulus was similar to the testing stimulus except that the left and right gratings had the same phase and contrast. Figure 1F depicts our observers' average results. Confirming the prediction, perceived contrast was lower with the D-MBC (1.39 $\pm$ 0.02 log unit, M + SE) than D-NS and D-BBC stimuli (1.68 $\pm$ 0.01 and 1.66 $\pm$ 0.01 log unit, respectively) [D-MBC versus D-NS: $t(4) = -18.52$ $p = 5.0 \times 10^{-5}$; D-MBC versus D-BBC: $t(4) = -22.36$, $p = 2.4 \times 10^{-5}$].

We also tested two monocular stimuli as controls, which we call the monocular-NS (Figure 1D) and monocular-MBC (Figure 1E) conditions. We found perceived contrast in D-MBC stimulus was slightly higher but close to both control conditions [D-MBC versus M-NS: $t(4) = 4.95$ $p = 0.008$; D-MBC versus M-MBC: $t(4) = 4.06$ $p = 0.015$]. This indicates the uniform grating in D-MBC (right half-image in Figure 1B)

contributed little to perceived contrast. One explanation for this is that the eye receiving the MBC grating square exerted stronger interocular suppression onto the uniform grating. This is reminiscent of our previous binocular rivalry (BR) studies using an MBC-BR stimulus (Figure 2A), where the MBC disc (vertical grating) half-image largely dominates over the corresponding uniform horizontal grating half-image (Ooi and He, 2006; Su et al., 2009, 2011a, 2011b; Xu et al., 2010). Nonetheless, we recognized that the D-MBC stimulus (Figure 1B) differs from the MBC-BR stimulus in that the grating orientation in the two eyes are similar in the former, and, thus, fusible. To support our hypothesis that the uniform grating in D-MBC was also interocularly suppressed, **Experiment 2** measured increment thresholds for detecting a monocular Gabor probe in the D-MBC stimulus (Figure 2B). The left pair in Figure 2B shows a Gabor probe being presented against the MBC grating disc pedestal (1.0 log unit), whereas the right pair shows the probe being presented against the uniform grating pedestal (1.6 log unit). We predicted that should the uniform grating be suppressed, detection threshold would be higher in the scenario of Figure 2B right pair than left pair (Su et al., 2009, 2010). We measured our observers' thresholds using a combined 2AFC and QUEST method and found the average threshold (circles in Figure 2E) was indeed higher on the uniform grating pedestal [1.37 $\pm$ 0.05 vs. 0.91 $\pm$ 0.03 log unit; $t(3) = 15.33$; $p = 6.02 \times 10^{-4}$].

In addition, we tested two control stimuli, the D-NS (Figure 2C) and D-BBC/ring (Figure 2D) stimuli, to rule out the confounding factor that the lower contrast pedestal of the MBC disc caused the lower detection threshold. If the higher threshold on the uniform grating in D-MBC (Figure 2B, right pair) was merely due to a higher pedestal contrast, we should expect similar high thresholds with the D-NS (Figure 2C, right pair) and D-BBC/ring (Figure 2D, right pair) stimuli. But this prediction was not borne out. As shown in Figure 2E, with the higher contrast pedestal being 1.6 log unit, the average probe threshold was significantly higher with the D-MBC stimulus (circular symbol) than with either the D-NS [$t(3) = 8.07$, $p = 0.004$] or D-BBC/ring [$t(3) = 5.37$, $p = 0.013$] stimuli. Further, for both control stimuli, the average probe thresholds did not differ significantly between the two contrast pedestals [D-NS: square symbol, $t(3) = 1.97$; $p = 0.144$; D-BBC/ring: triangular symbol, $t(3) = 0.37$; $p = 0.738$]. Also, with the lower contrast pedestal, the average probe threshold was significantly lower with the D-MBC stimulus than with the D-NS stimuli [$t(3) = -8.01$, $p = 0.004$] and D-BBC/ring [$t(3) = -7.55$, $p = 0.005$]. This suggests that in comparison against the D-NS and D-BBC/ring stimuli, the lower increment contrast threshold measured on the half-image with MBC in the D-MBC stimulus was due to reduced suppression from the fellow eye.

Experiments 1 and 2 together revealed that with the D-MBC stimulus, the visual system represents the MBC grating while suppressing the uniform grating (without BC) in the fellow eye even when the two gratings are fusible. But what happens when the two eyes receive BC of different strengths? To answer this, **Experiment 3** capitalized on the D-BBC stimulus to measure how having an interocular BC strength ratio affected binocular contrast integration. Recall we created the BCs of the dichoptic stimuli in Experiment 1 by adding surround gratings of different phases (Figure 1). Similarly, the current experiment used a series of set phases (-45, -75, -90, -105, -120, -135, -180 deg) to manipulate the interocular BC strength ratio (Table S2). For example, the stimulus in Figure 3A is modified from the D-MBC stimulus (Figure 1B) by replacing the $-45°$ surround grating with a $-75°$ surround. This causes a significant increase of BC strength in the right half-image and hence changes the BC strength ratio between the right (high-contrast central grating) and left (low-contrast central grating) half-images. We then conducted two measurements. One, we measured perceived contrast of the various D-BBC stimuli using the same contrast matching task as in Experiment 1. Two, we measured observers' perceived strength (saliency) of the BC in each half-image by rating it from a scale of 0–10. This allows us to calculate the perceived interocular BC strength ratios between the right and left half-images. Figure 3B plots the average perceived contrast (y axis) against the perceived interocular BC strength ratio (x axis). Clearly, perceived contrast varied significantly with the perceived interocular BC strength ratio [$F(6, 21) = 10.70$; $p = 1.8 \times 10^{-5}$; One way ANOVA with repeated measures]. The data were fitted by the curve, $b + a \times \frac{1}{2}\left[1 + \mathrm{erf}\left(\frac{x-\mu}{\sigma\sqrt{2}}\right)\right]$. The finding that perceived contrast increases with the interocular BC strength ratio indicates that BC strengths, besides grating contrast, contributes to binocular contrast integration of D-BBC stimuli.

Experiment 4 generalized our conclusion by extending to another aspect of perceived spatial feature of the interior surface, namely, its spatial phase. We modified the stimuli in Experiment 1 by assigning all gratings with a contrast of 1.5 log unit (Figure 4). With free fusion of the D-NS stimulus in Figure 4A, an observer with balanced eyes perceives the cyclopean grating has zero phase, ie, its darkest zone is aligned with the

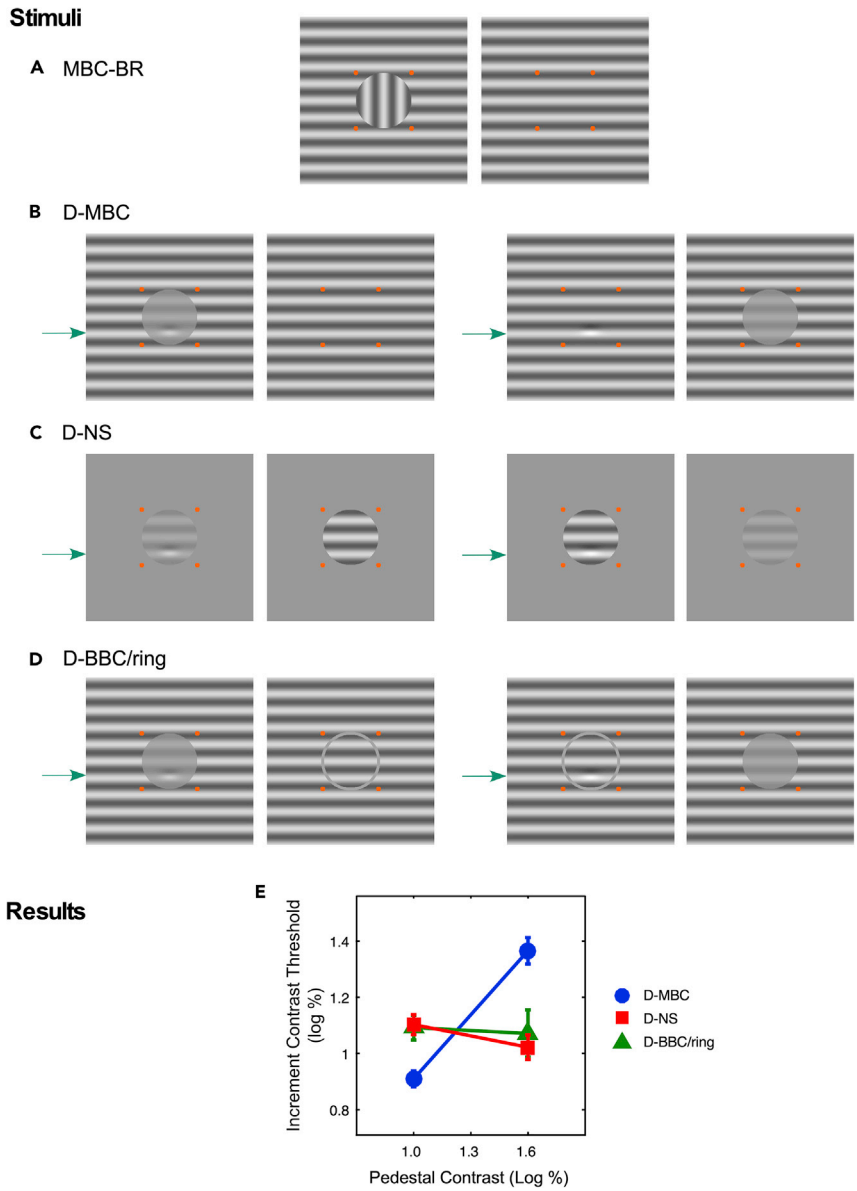

Figure 2. Experiment 2: Influence of BC on Increment Contrast Threshold Measured with a Gabor Probe

(A) An example of an MBC-BR stimulus with orthogonal orientation features in each eye.

(B–D) The three types of stimuli tested. For each dichoptic pair, increment contrast threshold was measured by the Gabor probe (as pointed to by green arrows) that is depicted in one half-image.

(E) Average results (n = 4) showing the average increment contrast threshold for seeing the Gabor probe as a function of pedestal contrast. Notably, when the pedestal was 1.6 log unit, threshold is highest in the D-MBC condition indicating suppression of the homogeneous grating (1.6 log unit) by the MBC half-image with low contrast (1.0 log unit) in the fellow eye. We defined perceived contrast in log unit. Therefore, the labeled y axis values of 1.4, 1.2, 1.0, and 0.8 correspond to 25.1%, 15.9%, 10%, and 6.3%, respectively. The error bars represent standard errors of the mean.

green reference lines. This confirms the cyclopean grating's phase is the mean phase of the two gratings from the two eyes [i.e., (−45° + 45°)/2 = 0°] (Badcock and Derrington, 1987; Ding et al., 2013; Ding and Sperling, 2006; Han et al., 2018; Huang et al., 2010). However, in Figure 4B, the perceived phase of the D-MBC stimulus is no longer zero but at a positive phase where the darkest zone of the cyclopean grating is above the reference lines. In fact, the perceived phase appears similar to that of the MBC grating in the left half-image. This observation resembles the perceived cyclopean contrast results of Experiment 1 where the contrast of the MBC grating dictated the perceived contrast. Also similar to Experiment 1, for the

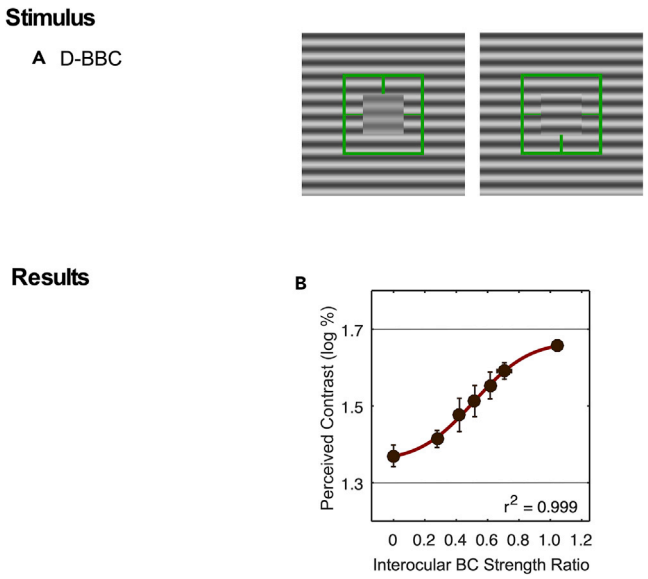

Figure 3. Experiment 3: Interocular BC Saliency Affecting Binocular Contrast Integration

(A) A sample stimulus showing a pair of half-images with different relative phase shifts between the central and surround gratings creating unequal BC saliency in each half-image. The contrast of the central grating with the higher BC saliency (left half-image) is lower than that in the fellow (right) half-image. See Transparent Methods and Table S2 for detailed descriptions of stimuli.

(B) Average results (n = 4) showing the perceived contrast as a function of interocular BC strength ratio between the central square grating with high contrast and central square grating with low contrast (filled symbols). The curve fitting the data is derived from observers' ratings of the BC saliency. Perceived binocular contrast is higher, which is largely contributed by the high-contrast grating (right), when the high-contrast grating's BC strength is about the same as that of the low contrast grating (left) (ratio = 1). We defined perceived contrast in log unit. Therefore, the labeled y axis values of 1.7, 1.5, and 1.3 correspond to 50.1%, 31.6%, and 20.0%, respectively. Both the vertical and horizontal error bars represent standard errors of the mean.

D-BBC stimulus, perceived cyclopean phase of the grating is almost zero, similar to the D-NS stimulus. We empirically verified these observations by measuring the perceived cyclopean phases of the central grating square of the D-NS, D-MBC, and D-BBC stimuli (Figures 4A–4C). Figure 4F depicts the average results showing perceived phase of the central grating in the D-MBC stimulus (above 45°) differed significantly from those in the D-NS and D-BBC stimuli [D-MBC versus D-NS: $t(4) = 41.72$, $p = 2.0 \times 10^{-6}$; D-MBC versus D-BBC: $t(4) = 39.48$, $p = 2.5 \times 10^{-6}$], indicating the effect of BC on binocular phase integration. As in Experiment 1, we tested two monocular control conditions, M-NS (Figure 4D) and M-MBC (Figure 4E). We found perceived phase in M-MBC was not significantly different from D-MBC ($t(4) = -2.14$; $p = 0.10$). This further confirms perceived cyclopean phase of the grating in D-MBC was dictated by the MBC grating. Curiously, we found perceived phase in the M-MBC stimulus was significantly larger than that in M-NS ($t(4) = 5.64$; $p = 0.005$). This suggests a phase-repulsion phenomenon between the central and surround gratings of different spatial phases.

DISCUSSION

Our results indicate binocular BC signals influence perceived cyclopean surface features (contrast and phase) of a grating surface. In the limiting case where one eye sees a BC-defined grating patch and the fellow eye sees the grating with the same orientation but without BC, the observer perceives predominantly the MBC grating patch alone. In other scenarios where there are BCs in both half-images, the interocular BC strength ratio affects the perceived cyclopean contrast of the grating surface. And in the case where the BCs in the two eyes have similar strengths (e.g., when interocular BC strength ratio is unity in Experiment 3), the high-contrast grating dominates the cyclopean contrast perception. In other words, both the interocular BC and local contrast signals determine the perceived interior features of a surface.

The current finding that BC influences the perception of a surface's interior supports the notion that surface representation begins at the BC. It is also consistent with our previous studies using binocular rivalry stimuli

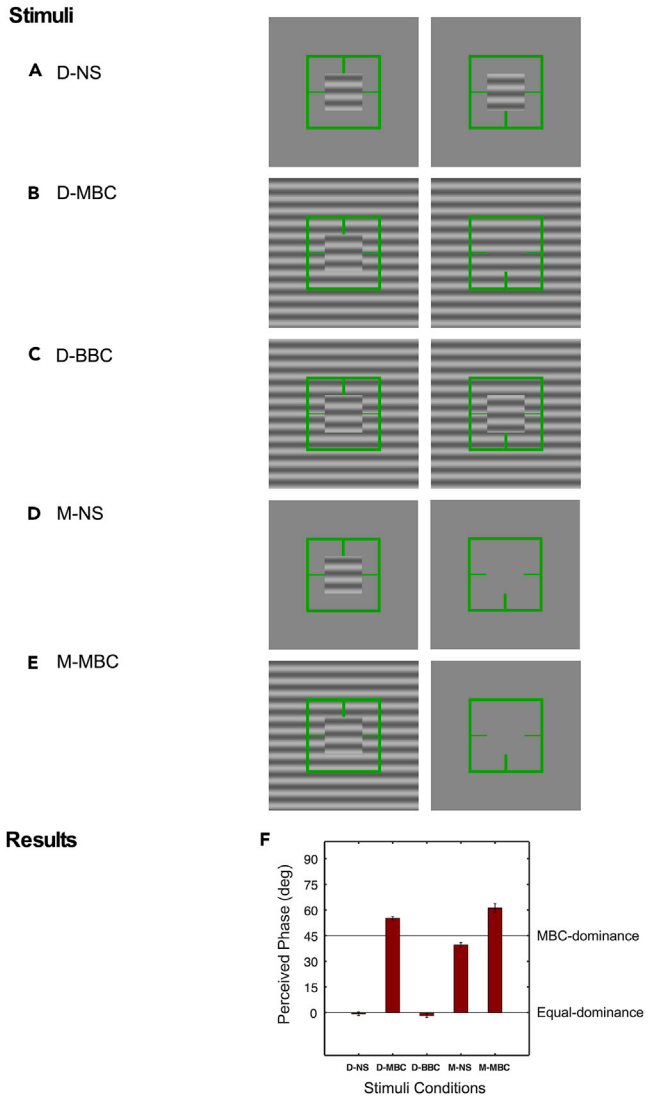

Figure 4. Experiment 4: Influence of BC on Phase Integration

(A–E) The stimuli were the same as those in Experiment 1 except that all gratings had a contrast of 1.5 log unit.

(F) Results showing the average perceived binocular phase in the five conditions. Notably, perceived phase in the D-MBC condition is higher than in the D-NS condition, indicating the role of BC (n = 5). The error bars represent standard errors of the mean.

(Su et al., 2010, 2011a, 2011b; Xu et al., 2010, 2016). We showed with non-fusible binocular rivalry (BR) stimulus that the visual system first registers the BC, before the local texture region adjacent to the BC, for determination of the dominant surface (Su et al., 2011a, 2011b). In one study (Su et al., 2011b), we presented an MBC-BR stimulus similar to that in Figure 2A, except for the MBC being rectangular in shape and its texture horizontal-grating, to the observers for varying durations (30–500 ms). The fellow eye received a vertical-grating half-image. We then asked observers to report the pattern of the textures (vertical, horizontal, or checkerboard) they saw in the rectangular area interior to the MBC. Our data showed at short durations, observers saw the (dominant) horizontal grating adjacent to the MBC, whereas the central area of the MBC rectangle was filled with checkerboard texture. With longer presentation durations, the coverage of the dominant horizontal grating spread toward the center while the central checkerboard area shrank, until the entire MBC rectangle was covered with the dominant grating. We then calculated the speed of filling-in and found it to be constant when scaled according to cortical distance in the early visual cortical areas (V1 and V2). Of significance, the current study supports a similar border-to-interior strategy for

representing texture surface with fusible features (same orientation). Here, we further showed perceived binocular surface's (e.g., interior contrast perception) dependence on both local contrast and BC signals (Figure 3). In the case of the D-MBC stimulus, the cyclopean percept of the interior surface (grating) is mainly contributed by the half-image with the BC.

Although there is yet no neurophysiological evidence directly showing how the *border-to-interior representation* strategy is implemented to represent textured-surfaces, there are empirical findings suggesting the involvement of both top-down cortical feedback networks and bottom-up visual information. Based on these studies, it is reasonable to posit the *border-to-interior representation* strategy requires an image's border ownership (BC) to be determined before the texture and color fill-in the interior of the surface. The border-ownership selective neurons in V2 are likely modulated by feedbacks from higher-level visual cortical areas where characteristics of global surface properties, 3-D surface layouts, and natural objects are represented (Chen et al., 2014; Craft et al., 2007; Hesse and Tsao, 2016; Ko and von der Heydt, 2018; Lamme and Roelfsema, 2000; Qiu et al., 2007; Qiu and von der Heydt, 2005; von der Heydt, 2015; von der Heydt and Zhang, 2018; von der Heydt et al., 2000; Williford and von der Heydt, 2016; Zhou et al., 2000). In addition, these V2 neurons receive bottom-up local feature information, such as T-junctions and binocular disparity (Qiu and von der Heydt, 2005; von der Heydt and Zhang, 2018). For example, Qiu and von der Heydt found the V2 neurons' depth sign (selectivity) of border ownership was consistent with their depth sign (selectivity) revealed with RDS stimuli (Qiu and von der Heydt, 2005; von der Heydt et al., 2000). Presumably, the border-ownership selective neurons can carry surface texture and color features to initiate the filling-in process from the borders. This being the case, it requires a battery of border-ownership selective neurons having tuning functions to represent various types of texture patterns and colors. Indeed, single-unit recording studies of V2 neurons have revealed neural activities of border-ownership selective neurons are affected by surface texture and color features (Hesse and Tsao, 2016; Zhou et al., 2000). This further suggests border ownership is determined by a population of neurons distributed along the visual pathways (Hesse and Tsao, 2016; Ko and von der Heydt, 2018). It would be interesting for future studies to investigate whether the border ownership selective neurons directly participate in the filling-in process. In addition, our previous psychophysical findings as well as those of the current Experiment 2 have led us to hypothesize that the V2 border ownership neurons play a broader role in mediating interocular suppression to represent a global binocular surface, by integrating the often times ambiguous information from the two eyes (Ooi and He, 2006; Su et al., 2009, 2011a, 2011b; Xu et al., 2010).

The *border-to-interior representation* strategy notwithstanding, there is evidence that the binocular visual system is capable of representing surfaces devoid of BC information by employing the *region-based coding* strategy. In fact, much research has shown computer-generated RDS images can lead to 3-D surface perception (Julesz, 1960). Nevertheless, there are advantages in adopting a *border-to-interior representation* strategy to represent natural surfaces. This is because most natural surfaces are smooth, with abrupt surface discontinuation or curvature changes only occurring at their borders. As a consequence, useful information regarding the overall 3-D surface attributes pertaining to surface shapes and depth discontinuities are carried by BCs (Grossberg and Mingolla, 1985; Nakayama and Shimojo, 1990). One could further speculate that in the natural scene, it is arguably more efficient for the visual system to first find the corresponding BCs from the two eyes and then within each corresponding binocular BC to match the local features in the two eyes and compute their binocular depth relationship. In fact, a number of stereoscopic depth studies have shown that BCs can be critical in determining 3-D surface representation (He and Ooi, 2000; McKee, 1983; Mitchison and McKee, 1990; Ramachandran and Cavanaugh, 1985; Richards, 1977; Su et al., 2009). In addition, the color and texture of the surface region adjacent to the BC usually provides a good estimate of the entire surface, as the interior of most natural surfaces have common optical properties of color and texture (Elder and Goldberg, 2002; Fine et al., 2003). Moreover, neurophysiological studies have showed that V2 neurons with border ownership selectivity respond to both binocular depth discontinuities and luminance BC (Hesse and Tsao, 2016; Qiu and von der Heydt, 2005; von der Heydt, 2015; von der Heydt et al., 2000; Zhou et al., 2000). Consequently, using the border-to-interior strategy could optimize the efficiency of representing the interior structures of natural surfaces. In other words, the choice of representing binocular surfaces using the border-to-interior strategy among other possible strategies reflects the visual system's preference to utilize the ecological constraints inherent in natural scenes (Gillam and Borsting, 1988; Nakayama et al., 1995; Ooi and He, 2005; Paffen et al., 2006; Shimojo and Nakayama, 1990; van Bogaert et al., 2008).

Resource Availability

Lead Contact

Further information and requests for resources should be directed to and will be fulfilled by the Lead Contact, Teng Leng Ooi (ooi.22@osu.edu).

Materials Availability

This study did not generate new materials.

Data and Code Availability

The experimental code and data that support the findings of this study are available from our repository (GitHub: https://github.com/V-sci/BC_contrast-phase).

METHODS

All methods can be found in the accompanying Transparent Methods supplemental file.

SUPPLEMENTAL INFORMATION

Supplemental Information can be found online at https://doi.org/10.1016/j.isci.2020.101394.

ACKNOWLEDGMENTS

This study was supported by grants from the National Institutes of Health, United States (EY023561 and EY023374) to T.L.O. and Z.J.H.

AUTHOR CONTRIBUTIONS

Conceptualization: T.L.O. & Z.J.H.; Designed experiments: C.H., W.H., Y.R.S., Z.J.H., & T.L.O.; Performed the research: C.H., W.H., Y.R.S., & T.L.O: Analyzed the data: C.H., W.H., Y.R.S., Z.J.H., & T.L.O.; Writing: T.L.O., Z.J.H., C.H., & W.H.; Funding acquisition: T.L.O. & Z.J.H.

DECLARATION OF INTERESTS

The authors declare no competing interests.

Received: March 27, 2020
Revised: June 24, 2020
Accepted: July 17, 2020
Published: August 21, 2020

REFERENCES

Badcock, D.R., and Derrington, A.M. (1987). Detecting the displacements of spatial beats: a monocular capability. Vis. Res. *27*, 793–797.

Bakin, J.S., Nakayama, K., and Gilbert, C.D. (2000). Visual responses in monkey areas V1 and V2 to three-dimensional surface configurations. J. Neurosci. *20*, 8188–8198.

Chen, M., Yan, Y., Gong, X., Gilbert, C.D., Liang, H., and Li, W. (2014). Incremental integration of global contours through interplay between visual cortical areas. Neuron *82*, 682–694.

Craft, E., Schutze, H., Niebur, E., and von der Heydt, R. (2007). A neural model of figure-ground organization. J. Neurophysiol. *97*, 4310–4326.

Ding, J., Klein, S.A., and Levi, D.M. (2013). Binocular combination of phase and contrast explained by a gain-control and gain-enhancement model. J. Vis. *13*, 13.

Ding, J., and Sperling, G. (2006). A gain-control theory of binocular combination. Proc. Natl. Acad. Sci. U S A. *103*, 1141–1146.

Duncan, R.O., Albright, T.D., and Stoner, G.R. (2000). Occlusion and the interpretation of visual motion: perceptual and neuronal effects of context. J. Neurosci. *20*, 5885–5897.

Elder, J.H., and Goldberg, R.M. (2002). Ecological statistics of Gestalt laws for the perceptual organization of contours. J. Vis. *2*, 324–353.

Fine, I., MacLeod, D.I., and Boynton, G.M. (2003). Surface segmentation based on the luminance and color statistics of natural scenes. J. Opt. Soc. Am. A. Opt. Image Sci. Vis. *20*, 1283–1291.

Georgeson, M.A., Wallis, S.A., Meese, T.S., and Baker, D.H. (2016). Contrast and lustre: a model that accounts for eleven different forms of contrast discrimination in binocular vision. Vis. Res. *129*, 98–118.

Gillam, B., and Borsting, E. (1988). The role of monocular regions in stereoscopic displays. Perception *17*, 603–608.

Grossberg, S., and Mingolla, E. (1985). Neural dynamics of form perception: boundary completion, illusory figures, and neon color spreading. Psychol. Rev. *92*, 173–211.

Halpern, D.L., and Blake, R.R. (1988). How contrast affects stereoacuity. Perception *17*, 483–495.

Han, C., He, Z.J., and Ooi, T.L. (2018). On sensory eye dominance revealed by binocular integrative and binocular competitive stimuli. Invest. Ophthalmol. Vis. Sci. *59*, 5140–5148.

He, Z.J., and Ooi, T.L. (2000). Perceiving binocular depth with reference to a common surface. Perception *29*, 1313–1334.

Hesse, J.K., and Tsao, D.Y. (2016). Consistency of border-ownership cells across artificial stimuli,

natural stimuli, and stimuli with ambiguous contours. J. Neurosci. *36*, 11338–11349.

Hou, F., Huang, C.B., Liang, J., Zhou, Y., and Lu, Z.L. (2013). Contrast gain-control in stereo depth and cyclopean contrast perception. J. Vis. *13*, 1–19.

Huang, C.B., Zhou, J., Zhou, Y., and Lu, Z.L. (2010). Contrast and phase combination in binocular vision. PLoS One *5*, e15075.

Julesz, B. (1960). Binocular depth perception of computer-generated patterns. Bell Syst. Tech. J. *39*, 1125–1162.

Ko, H.K., and von der Heydt, R. (2018). Figure-ground organization in the visual cortex: does meaning matter? J. Neurophysiol. *119*, 160–176.

Lamme, V.A., and Roelfsema, P.R. (2000). The distinct modes of vision offered by feedforward and recurrent processing. Trends Neurosci. *23*, 571–579.

Legge, G.E., and Gu, Y.C. (1989). Stereopsis and contrast. Vis. Res. *29*, 989–1004.

Marr, D., and Poggio, T. (1976). Cooperative computation of stereo disparity. Science *194*, 283–287.

McKee, S.P. (1983). The spatial requirements for fine stereoacuity. Vis. Res. *23*, 191–198.

Mitchison, G.J., and McKee, S.P. (1990). Mechanisms underlying the anisotropy of stereoscopic tilt perception. Vis. Res. *30*, 1781–1791.

Mumford, D., Kosslyn, S.M., Hillger, L.A., and Herrnstein, R.J. (1987). Discriminating figure from ground: the role of edge detection and region growing. Proc. Natl. Acad. Sci. U S A *84*, 7354–7358.

Nakayama, K., He, Z.J., and Shimojo, S. (1995). Visual surface representation: a critical link between lower-level and higher-level vision. In An Invitation to Cognitive to Cognitive Science: Visual Cognition, S.M. Kosslyn and D.N. Osherson, eds. (MIT Press), pp. 1–70.

Nakayama, K., and Shimojo, S. (1990). Toward a neural understanding of visual surface representation. In The Brain, Cold Spring Harbor Symposium on Quantitative Biology, *55*, T. Sejnowski, E.R. Kandel, C.F. Stevens, and J.D. Watson, eds. (Cold Spring Harbor Laboratory), pp. 911–924.

Ohzawa, I., DeAngelis, G.C., and Freeman, R.D. (1990). Stereoscopic depth discrimination in the visual cortex: neurons ideally suited as disparity detectors. Science *249*, 1037–1041.

Ooi, T.L., and He, Z.J. (2005). Surface representation and attention modulation mechanisms in binocular rivalry. In Binocular Rivaly, D. Alais and R. Blake, eds. (MIT Press), pp. 117–135.

Ooi, T.L., and He, Z.J. (2006). Binocular rivalry and surface-boundary processing. Perception *35*, 581–603.

Paffen, C.L., Tadin, D., te Pas, S.F., Blake, R., and Verstraten, F.A. (2006). Adaptive center-surround interactions in human vision revealed during binocular rivalry. Vis. Res. *46*, 599–604.

Paradiso, M.A., and Nakayama, K. (1991). Brightness perception and filling-in. Vis. Res. *31*, 1221–1236.

Poggio, G.F., and Fischer, B. (1977). Binocular interaction and depth sensitivity in striate and prestriate cortex of behaving rhesus monkey. J. Neurophysiol. *40*, 1392–1405.

Qiu, F.T., Sugihara, T., and von der Heydt, R. (2007). Figure-ground mechanisms provide structure for selective attention. Nat. Neurosci. *10*, 1492–1499.

Qiu, F.T., and von der Heydt, R. (2005). Figure and ground in the visual cortex: v2 combines stereoscopic cues with gestalt rules. Neuron *47*, 155–166.

Ramachandran, V.S., and Cavanaugh, P. (1985). Subjective contours capture stereopsis. Nature *317*, 257–530.

Richards, W. (1977). Stereopsis with and without monocular contours. Vis. Res. *17*, 967–969.

Shimojo, S., and Nakayama, K. (1990). Real world occlusion constraints and binocular rivalry. Vis. Res. *30*, 69–80.

Su, Y., He, Z.J., and Ooi, T.L. (2009). Coexistence of binocular integration and suppression determined by surface border information. Proc. Natl. Acad. Sci. U S A *106*, 15990–15995.

Su, Y.R., He, Z.J., and Ooi, T.L. (2010). The magnitude and dynamics of interocular suppression affected by monocular boundary contour and conflicting local features. Vis. Res. *50*, 2037–2047.

Su, Y.R., He, Z.J., and Ooi, T.L. (2011a). Revealing boundary-contour based surface representation through the time course of binocular rivalry. Vis. Res. *51*, 1288–1296.

Su, Y.R., He, Z.J., and Ooi, T.L. (2011b). Seeing grating-textured surface begins at the border. J. Vis. *11*, 14.

van Bogaert, E.A., Ooi, T.L., and He, Z.J. (2008). The monocular-boundary-contour mechanism in binocular surface representation and suppression. Perception *37*, 1197–1215.

von der Heydt, R. (2015). Figure-ground organization and the emergence of proto-objects in the visual cortex. Front. Psychol. *6*, 1695.

von der Heydt, R., and Zhang, N.R. (2018). Figure and ground: how the visual cortex integrates local cues for global organization. J. Neurophysiol. *120*, 3085–3098.

von der Heydt, R., Zhou, H., and Friedman, H.S. (2000). Representation of stereoscopic edges in monkey visual cortex. Vis. Res. *40*, 1955–1967.

Williford, J.R., and von der Heydt, R. (2016). Figure-ground organization in visual cortex for natural scenes. eNeuro *3*, 1–15.

Xu, H., Han, C., Chen, M., Li, P., Zhu, S., Fang, Y., Hu, J., Ma, H., and Lu, H.D. (2016). Rivalry-like neural activity in primary visual cortex in anesthetized monkeys. J. Neurosci. *36*, 3231–3242.

Xu, J.P., He, Z.J., and Ooi, T.L. (2010). Surface boundary contour strengthens image dominance in binocular competition. Vis. Res. *50*, 155–170.

Zhou, H., Friedman, H.S., and von der Heydt, R. (2000). Coding of border ownership in monkey visual cortex. J. Neurosci. *20*, 6594–6611.

iScience, Volume *23*

Supplemental Information

Evidence in Support of the Border-Ownership Neurons for Representing Textured Figures

Chao Han, Wanyi Huang, Yong R. Su, Zijiang J. He, and Teng Leng Ooi

Supplemental Information

Transparent Methods

Observers

A total of nine observers who were naïve to the purpose of the study and two authors participated in the various experiments. Of these, four naïve observers and one author participated in Experiments 1 and 4. Three new naïve observers and another author participated in Experiment 2. Experiment 3 tested two naïve observers who also participated in Experiments 1 and 4 and two other new naïve observers.

All observers had normal or corrected-to-normal visual acuity (at least 20/20), clinically acceptable fixation disparity (≤8.6 arc min) and stereopsis (≤40 arc sec). The research conducted followed the tenets of the Declaration of Helsinki and was approved by the institutional review board (IRB). Informed consent was obtained from the observers after explanation of the nature and possible consequences of the study.

Apparatus

Gamma corrected stimuli were generated either on a PC (Linux) or Mac Pro computer running MatLab with PsychToolBox and presented on a 21-inch flat CRT monitor (Brainard, 1997; Pelli, 1997). The resolution of the monitor was 2048 × 1536 pixels @ 75 Hz. During the experiments, except for Experiment 3b, the observers viewed the computer monitor through a haploscopic mirror system attached to a head-and-chin rest to assist fusion of the dichoptic stimuli from a distance of 100 cm. From this viewing distance the entire screen had an angular dimension of 23^{o} horizontally and 17.3^{o} vertically. The screen was halved by the haploscopic mirror system,

resulting in each eye having a field of view of 11.5° by 17.3°. Experiment 3b was performed with unaided binocular viewing while observers steadied their head on the head-and-chin rest.

Experiment 1: BC influence on binocular contrast integration

Stimulus

The horizontal gratings in all five stimulus designs in figure 1 were 3cpd and 35 cd/m^2. The stimuli differed mainly in whether the small central grating square (1° × 1°) was shown against a larger surround square (8° × 8°) with uniform gray or grating background, and whether the gratings were viewed with one or both eyes. Also common was the binocular green square outline (2° × 2°) with horizontal reference lines (length=0.5° & width= 0.0112°, luminance=72 cd/m^2, CIE-1931: x = 0.29, y = 0.59) encircling the location of the central grating square serving as the fusion lock. Attached to the green squares was a pair of vertical nonius lines (length=0.5° & width=0.0336°) to ensure accurate eye alignment.

Stimuli 1a-1c were created with horizontal gratings whose phases were shifted relative to the horizontal green reference lines. The phases of the central square and surround gratings for the left and right half-images are shown in Table S1. The contrast of the central grating in one-half image (left in figure 1) was always 1.3 log unit while it was 1.7 log unit for all gratings in the other half-image. Stimuli 1d and 1e comprised the left half-images of stimuli 1a and 1b, respectively, and homogeneous gray field right half-images. During the experiment, for each stimulus type (1a-1e), the eye seeing the low contrast grating (left or right eye) and the phase shift direction (up or down) of the half-images were counterbalanced.

Procedures

We used the 2IFC method to measure perceived contrast of the central grating. In one interval, the test stimulus (fixed contrast, the test stimuli in figure 1) was presented and in the other interval the matching grating with variable contrast in the central square was presented. [The matching stimulus comprised a pair of dichoptic horizontal grating squares with a 90^o phase shift relative to the surrounding gratings, except for the D-NS and M-NS stimulus condition where only the central grating squares were presented without the surrounding gratings.] An audio sound (beep) accompanied each presentation interval. The observer prepared for a trial by aligning his/her eyes with the nonius lines attached to the green square. He/she then pressed a button on the keyboard to start the trial, which began with the presentation of interval-1 stimulus (400 ms), a blank interval (600 ms) and interval-2 stimulus (400 ms). A mask presentation (600 ms, 8^o × 8^o random dots patch, 50% black and 50% white, 35 cd/m^2, dot size = 4.7 arcmin, contrast = 1.7 log unit) indicated the end of the trial. He/she responded, by key press, whether the central grating contrast was higher in the first or second interval. We used the QUEST method to adjust the contrast of the matching grating until both gratings were perceived to be at the same contrast.

In the experiment, the eye seeing the low contrast grating (left or right eye) and the phase shift direction (up or down) of the half-images were counterbalanced, culminating in 20 stimulus combination [5 (stimuli types) × 2 (eyes) × 2 (phase direction) = 20]. Each stimulus combination was repeated two times for the stimuli in figure 1a-1c and 1e, and once for the stimulus in figure 1d. Additionally, the entire experiment was repeated twice, respectively, with the matching stimulus being presented in the second interval of the 2IFC protocol and in the first interval. Each QUEST block had 30 trials, ensuring sufficient repeats to obtain a stable result. There was a total of 2160 trials/subject [(4 (stimuli types) × 2 (repeats) + 1 (stimuli types) × 1 (repeat)] × 2 (eyes) ×

2 (phase direction) × 2 (interval) × 30 (trials per block)]. These trials were conducted over 2 sessions on different days. Each session took about 1.5 hours with breaks in between blocks.

Experiment 2: BC influence on probe sensitivity

Stimulus

The D-MBC stimulus (figure 2b left & right pairs) comprised a pair of dichoptic horizontal gratings (4.5° x 4.5°, 2.2 cpd) with 60 cd/m^2 mean luminance. One half-image had a homogeneous grating with 1.6 log unit contrast. The other half-image had the same grating with an additional 1.5° sinusoidal grating disc in the center with a contrast of 1.0 log unit. Four small dots (diameter=0.13°, luminance=55 cd/m^2 , CIE 0.46, 0.46) in a square formation (1.5° x 1.5°) in the center of each half-image served as the fusion lock. The D-NS stimulus (figure 2c left & right pairs) comprised a pair of dichoptic discs with the same grating parameters surrounded by a gray background (60 cd/m^2). The D-BBC/ring stimulus (figure 2d left & right pairs) was similar to the D-MBC stimulus except that a gray ring (62 cd/m^2, width = 0.0224 deg) was added to the half-image without the disc at the corresponding location.

We measured the contrast increment threshold of seeing a monocular Gabor probe presented on either half-image of the stimulus. The probe was specified by the following formula:

$$L(x,y) = L_m\{1 + \sin(2\pi\omega x) \cdot [c + a \cdot \exp(-\frac{x^2}{2 \cdot {\sigma_1}^2} - \frac{(y \pm 0.375)^2}{2 \cdot {\sigma_2}^2})]\}$$

In the formula, *L(x, y)* represents the luminance at the specified location (*x*, *y*). The *y*-axis is orthogonal to the orientation of the probe's pedestal grating while the *x*-axis is parallel with the grating orientation; the origin overlaps the center of the grating pedestal. L_m is the mean luminance (60 cd/m^2); *c* is the Michelson contrast of the grating, $(L_{max}-L_{min})/(L_{max}+L_{min})$; *a* is the peak contrast

increment of the probe (proportion). In this paper, both *c* and *a* are presented in log unit, ie, $\log_{10}(c*100)$ or $\log_{10}(a*100)$. ω is the spatial frequency of the grating (2.2 cpd); σ_1 and σ_2 are the standard deviations of the Gaussian function in the Gabor kernel on x- and y-axis (σ_1 was set to 0.1826° and σ_2 was set to 0.1062°). The location of the probe on the grating pedestal was either 0.375° above or below the center of the stimulus. The probe was always presented to the observer's non-dominant eye, and is depicted as a contrast increment on the left half-images of the stimuli in figure 2. Testing of increment contrast threshold was repeated 6 times for each stimulus, and the order of testing was pseudo-randomized.

Procedure

We used a 2AFC-QUEST design to determine the contrast threshold of the Gabor probe. To begin a trial, the observer steadied himself/herself on a head-and-chin rest and maintained eye alignment with the nonius fixation (0.45° x 0.45°, width=0.1°, 68 cd/m^2). He/she then pressed the spacebar on the keyboard to present the stimulus. Five hundred ms after the onset of the stimulus, a 250 ms Gabor probe was presented. The stimulus remained for another 500 ms before a 500 ms random-dot mask (4.5° × 4.5° random dots patch, 50% black and 50% white, 60 cd/m^2, dot size = 6.8 arcmin, contrast = 1.97 log unit) was displayed to end the trial. The observer's task was to report with key press whether the probe was above or below the stimulus' center. The observer then pressed the space bar to initiate the next trial. The probe contrast increment (log unit) in the subsequent trial was determined with the QUEST procedure. A total of 6 stimulus combinations were tested: 2 (probe on each half-image) x 3 (stimulus type). Each stimulus combination was tested 6 times. In each block, there were at least 30 trials, with the testing only ending when the standard deviation of the QUEST model was smaller than 0.05, or a maximum of 60 trials was reached. On average, each block had about 50 trials. For each subject, there were1800 trials [2

(probe on each half-image) x 3 (stimulus type) x 6 (repeated block) x 50 (trials per block)] that was conducted over 2 sessions. Each session took about 1.5 hours with breaks in between blocks.

Experiment 3: Binocular contrast integration with different interocular BC strength ratio

Stimulus

The current Experiment 3 tested observers in two different tasks: (a) 2IFC contrast matching task and (b) BC rating task. The stimuli were based on the D-BBC stimulus (figure 1c) design in Experiment 1. Basically, the phases of the surrounding gratings in the two half-images were successively shifted to generate six other pairs of stimuli (see Table S2: third and sixth columns). The BC created by the relative phase shift between the center and surrounding gratings in each half-image is quantified as the effective phase shifts (Table S2: fourth and seventh columns). The ratio of the right to left half-image's effective phase shift defines the BC ratio (Table S2: first column). A ratio of 0 and unity, respectively, defines the D-MBC (figure 1b) and D-BBC stimuli (figure 1c) used in this and Experiment 1.

Experiment 3a (contrast matching) used the test stimuli described in Table S2. The matching stimulus comprised a pair of dichoptic horizontal grating squares with a 90^{o} phase shift relative to the surrounding gratings. The stimulus parameters (size, duration, luminance and contrast) were the same as in Experiment 1. We tested 7 different BC ratios. The eye seeing the low contrast grating (left or right eye) and the phase shift direction (up or down) of the half-images were counterbalanced. The test grating was presented either in the first or second 2IFC interval (while the matching grating in the other interval), culminating in 56 stimulus combinations [7 (BC ratios) × 2 (eyes) × 2 (phase direction) × 2 (intervals) = 56]. Each stimulus combination was repeated 2 times, and each QUEST block had 30 trials. There was a total of 3360 trials (56 × 2 ×

30) for each subject, which were conducted over 2 sessions on different days. Each session took about 2 hours with breaks in between blocks.

Experiment 3b (BC rating) tested observers' perception of the BC saliency of each half-image. Thirteen sets of half-images were created by phase shifting the central grating relative to the surround to produce effective phase shifts of 0^o to 180^o in 15^o intervals. We reduced the size of the surrounding grating (4^o x 4^o) to allow all 13 test stimuli to be displayed simultaneously on the computer screen. Based on the 13 stimulus set, eight different stimulus combinations were tested to counterbalance for phase shift direction, contrast and MBC shape (square or circle). Specifically, the grating patches were shifted either upward or downward relative to the surround. The contrast of the central grating patches were either 1.3 or 1.7 log unit (the contrast of the surround gratings were always 1.7 log unit). The shapes of the grating patches were square for the first four stimulus combinations tested and circular for the last four stimulus combinations.

Procedure

3a: Contrast matching task

As in Experiment 1, we used a 2IFC procedure with the same temporal sequence to test suprathreshold contrast perception. The QUEST method adjusted the contrast of the matching stimulus after each trial. But unlike Experiment 1, we implemented two QUEST sequences in the same block of trials (rather than in different blocks). One QUEST sequence had the test stimulus in the first interval and the matching stimulus in the second interval, while the other sequence had the reverse order. A total of 28 stimulus combinations were tested: 7 (stimuli with different BC ratio) x 2 (phase direction) x 2 (eyes). Each stimulus combination was repeated 4 times.

3b: BC rating

We tested the perceived contour strength of the same observers who performed the contrast matching experiment with the perceptual rating task. To begin the task, two reference stimuli that were essentially each half-image of a D-BBC stimulus were shown to the observers. The half-image with the homogeneous grating was given a rating score of "0" indicating no perceptible BC in the central area of the grating, while the half-image with the central grating (MBC created by 180 degrees phase shift relative to surround) was given a score of "10" indicating a highly salient BC. Then the 13 test stimuli with different effective phase shifts were presented. The observers verbally rated the perceived BC strength of each stimulus and the experimenter recorded the data.

Experiment 4: BC influence on phase integration

Stimulus

The stimuli used (figure 4a-e) were the same as those in Experiment 1 (figure 1a-e) except that all gratings carried a contrast of 1.5 log unit.

Procedure

The observer prepared for a trial by maintaining accurate eye alignment on the green square. Then to begin the trial, he/she would press a button on the keyboard. This was followed 146 ms later, with the presentation of the grating stimulus for 400 ms. A mask ($8^o \times 8^o$ random dots patch, 50% black and 50% white, 35 cd/m^2, dot size = 4.7 arcmin, contrast = 1.7 log unit) was then presented for 200 ms and was followed by a gray background until the observer responded. The observer's task was to report by key press the perceived center of the central dark band of the grating as above or below the horizontal reference lines.

The phases of all gratings were simultaneously adjusted with the same magnitude after each trial until the spatial phase was perceived as centered on the reference lines, using a

1up/1down staircase procedure with 10 reversals in an experimental block. The mean of the last 6 reversals was recorded to calculate the perceived cyclopean phase. Depending on the eye (LE/RE) viewing the MBC grating disc and the direction (phase-above/phase-below) of the phase-shift, there were four stimulus combinations of the D-MBC, M-MBC and M-NS conditions, and two combinations of D-NS and D-BBC conditions (because LE_phase-above is the same as RE_phase-below against a neutral background, and vice versa). The order of testing all stimulus combinations was counterbalanced between blocks. Each stimulus combination was repeated 4 times for the D-MBC, M-MBC and M-NS, and 8 times for the D-NS and D-BBC stimuli. Each block took about 20 trials to finish the 10 staircase reversals. Thus, the total number of trials for each subject was about 1600 {[3 (conditions) × 2 (eyes) × 2 (phase direction) × 4 (repeats) + 2 (conditions) × 2 (eyes) ×8 (repeats)] * 20 (trials per block)}, which were finished in 1 session.

Supplementary references:

Brainard, D. H. (1997). The Psychophysics Toolbox. *Spat Vis*, 10, 433-436.

Pelli, D. G. (1997). The VideoToolbox software for visual psychophysics: transforming numbers into movies. *Spat Vis*, 10, 437-442.

Table S1. Related to Figure 1(a-e)

Stimulus	Left half-image		Right half-image	
	Center (1.3 log unit)	**Surround (1.7 log unit)**	**Center (1.7 log unit)**	**Surround (1.7 log unit)**
a. D-NS	+45	gray	-45	gray
b. D-MBC	+45	-45	-45	-45
c. D-BBC	+45	180	-45	180
d. M-NS	+45	gray	gray	gray
e. M-MBC	+45	-45	gray	gray

Table S2. Related to Figure 3(a)

BC ratio	Left half-image			Right half-image		
=R/L	**Center (1.3 log unit)**	**Surround (1.7 log unit)**	**Effective phase shift (L)**	**Center (1.7 log unit)**	**Surround (1.7 log unit)**	**Effective phase shift (R)**
0 (D-MBC)	+45	-45	90	-45	-45	0
0.25	+45	-75	120	-45	-75	30
0.33	+45	-90	135	-45	-90	45
0.4	+45	-105	150	-45	-105	60
0.45	+45	-120	165	-45	-120	75
0.5	+45	-135	180	-45	-135	90
1 (D-BBC)	+45	-180	135	-45	-180	135